

Numerical Study of Collective Formation Process of Fe-Al Alloy Nanoparticles in Thermal Plasma Tail Using Two-Component Co-condensation Model

S. Tsurumi¹, M. Sugimoto¹, M. Shigeta¹, Jian Wang² and Y. Hirayama²

¹ Department of Mechanical Systems Engineering, Graduate School of Engineering, Tohoku University, Miyagi, Japan

² Magnetic Powder Metallurgy Research Center, National Institute of Advanced Industrial Science and Technology, Aichi, Japan

Abstract: Numerical simulation was carried out to clarify the formation process of Fe-Al alloy nanoparticles and to predict the number density distribution of the finally synthesized nanoparticles. The results indicate that Al condensation is slower than Fe condensation, and at about 1700 K, both Fe and Al vapors are consumed and converted into particles. At the temperature of 1750 K, the nanoparticles with an Al content of 20 at.% and larger than about 180 nm are already solidified, while smaller particles are still in a liquid state.

Keywords: Thermal plasma, Fe-Al alloy, Nanoparticles, Co-condensation, Numerical analysis.

1. Introduction

Various nanoparticles exhibit new properties that are different from those of bulk materials. In particular, Fe-Al alloy nanoparticles have been reported to offer ferromagnetism above room temperature [1] and are expected to be a material with new magnetic properties. The radio-frequency induction thermal plasma (RFITP) process is attracting attention as a method to realize high-speed mass production of nanoparticles, because the process can evaporate raw materials by its impurity-free high-temperature plasma generated by electrodeless discharge and has a high cooling rate at the tail part of the plasma [2]. Experimental studies have been conducted to synthesize alloy nanoparticles using thermal plasma [3]. However, it is difficult to measure and observe the formation process of alloy nanoparticles from metal vapor through nucleation, co-condensation, and coagulation. Therefore, the detailed formation process of alloy nanoparticles has not yet been clarified. This study aims to clarify the formation mechanisms of Fe-Al alloy nanoparticles under a typical cooling condition in the downstream region of an RFITP and to predict the final particle diameter and composition distribution of the synthesized alloy nanoparticles by a numerical simulation using the mathematical model and the calculation algorithm developed by the authors originally [4].

2. Models of Nanoparticle Collective Formation

2.1 Two-Component Co-condensation Model

In this study, the computational model developed by Shigeta and Watanabe [4] was applied to the collective formation process of Fe-Al alloy nanoparticles during cooling to investigate the number density distribution of the nanoparticles on the particle diameter-composition plane. In this process, Fe vapor and Al vapor collectively form Fe-Al alloy nanoparticles. The particle diameter d and Al content x were respectively discretized into d_k and x_n , where k and n are natural numbers. The time evolution of the particle number density $N_{k,n}$ defined at each discrete point is described by the following equations:

$$\frac{dN_{k,n}}{dt} = [\dot{N}_{k,n}]_{\text{nucl}} + [\dot{N}_{k,n}]_{\text{cond}} + [\dot{N}_{k,n}]_{\text{coag}}, \quad (1)$$

$$[\dot{N}_{k,n}]_{\text{nucl}} = I^* \xi_k^{(\text{nucl})} \psi_n^{(\text{nucl})}, \quad (2)$$

$$[\dot{N}_{k,n}]_{\text{cond}} = \sum_i \sum_l \frac{(\xi_{i,l,k}^{(\text{cond})} \psi_{i,l,n}^{(\text{cond})} - \delta_{i,k} \delta_{l,n}) N_{i,l}}{\Delta t}, \quad (3)$$

and

$$[\dot{N}_{k,n}]_{\text{coag}} = \frac{1}{2} \sum_i \sum_j \sum_l \sum_m \xi_{i,j,k}^{(\text{coag})} \psi_{i,j,l,n}^{(\text{coag})} \beta_{i,j,l,m} N_{i,l} N_{i,m} - N_{k,n} \sum_i \sum_l \beta_{i,k,l,n} N_{i,l}, \quad (4)$$

where t is the time, Δt is the increment of the time step, \dot{N} is the net particle production rate, and the subscripts nucl, cond, and coag denote the contributions to the number density change due to the nucleation, condensation, and coagulation, respectively. I^* is the homogeneous nucleation rate. ξ and ψ are the splitting operators in the particle diameter and composition directions, respectively. The particle volume conservation is considered in the splitting operators. β is the collision frequency function and δ is the Kronecker delta.

2.2 Computational Conditions

In this study, the precursor powders consisting of Fe : Al = 3 : 1 were supplied at 0.27 g/min with Ar gas supplied at 3.0 L/min. The numerical calculation of the nanoparticle formation process at the plasma tail was started after all the powders were vaporized by the plasma and became a homogeneous vapor. The cooling rate was set to be 2.0×10^4 K/s as a typical condition at the plasma tail.

2.3 Melting Point Depression

The particle size dependence on the melting point T_{MP} of metal particles due to the Gibbs-Thomson effect was also considered by the following equations [5]:

$$T_{MP,k,n} = T_{MP,bulk} \left(1 - \frac{\alpha'_n}{d_k} \right), \quad (5)$$

and

$$\alpha'_n = (1 - x_n)\alpha_{(Fe)} + x_n\alpha_{(Al)}, \quad (6)$$

where α is a parameter determined by the surface energy of the solid and liquid and the melting enthalpy of the bulk material. In this study, the values in Ref. [5] were used. $T_{MP,bulk}$ is the melting temperature of the bulk and depends on the Al content in the Fe-Al alloy. $T_{MP,bulk}$ was calculated from the temperature on the solid phase curve in the phase diagram [6].

3. Results and Discussion

Figure 1 shows the number density distribution of Fe-Al alloy nanoparticles at 300 K. The majority of the produced particles had the Al content of about 25 at.%. This result suggests that nanoparticles with a composition which is approximately equal to the atomic number ratio of Fe and Al supplied as the raw materials can be obtained. On the other hand, the particle diameters varied widely ranging from a few nm to over 100 nm.

Figure 2 shows the vapor consumption rates due to nucleation and condensation of Fe and Al during the cooling process. The simultaneous nucleation processes of both Fe and Al took place significantly at about 2200 K. The vapor consumption rates due to condensation were greater than those due to the nucleation for both vapors. Figure 3 shows the conversion ratios of Fe and Al vapors. Figure 4 shows a two-dimensional contour map of the Fe-Al alloy particle number density according to the particle diameter and Al content at 1750 K, where the black line shows the melting curve. Figure 3 shows that Al vapor condensed slower than Fe vapor. Moreover, at 2000 K, about 98% of the Fe vapor was consumed and converted to particles, while only about 60% of the Al vapor was consumed. Figure 4 shows that the nanoparticles with the Al content of 20 at.% and larger than about 180 nm were already solidified, while smaller particles were still in a liquid state. By comparing Fig. 3 with Fig. 4, in the region where the temperature was lower than 1750 K, the Al vapor condensed mostly into the solid particles larger than 180 nm.

4. Conclusion

In this study, the number density distribution of Fe-Al alloy nanoparticles which was synthesized using the RFITP was predicted. The formation process was also clarified by the numerical analysis. The number density distribution of the finally synthesized nanoparticles suggested that the composition of the nanoparticles was almost the same as the atomic number ratio of the raw materials. On the other hand, the particle diameters ranged from a few nm to larger than 100 nm. In the formation process, both Fe and Al nucleated at about 2200 K, and the vapor consumption rates by condensation were larger than

those by nucleation. In the condensation process, the Fe vapor condensed on the already existing nuclei earlier, followed by the Al vapor. The Al vapor

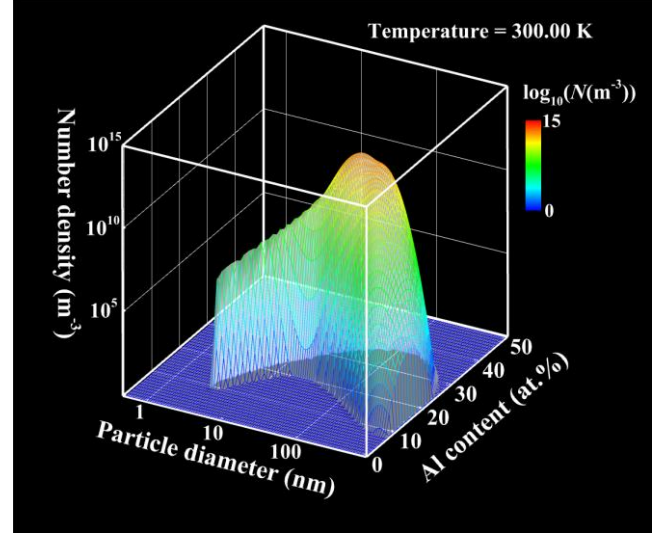


Fig. 1. Number density distribution of Fe-Al alloy particles at 300 K.

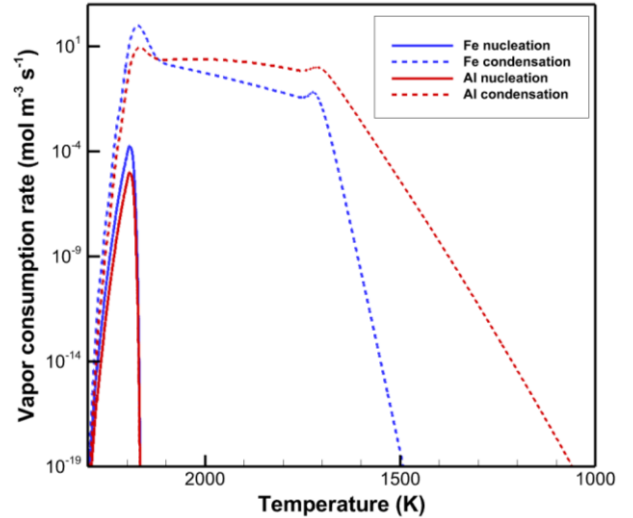


Fig. 2. Vapor consumption rates of Fe and Al.

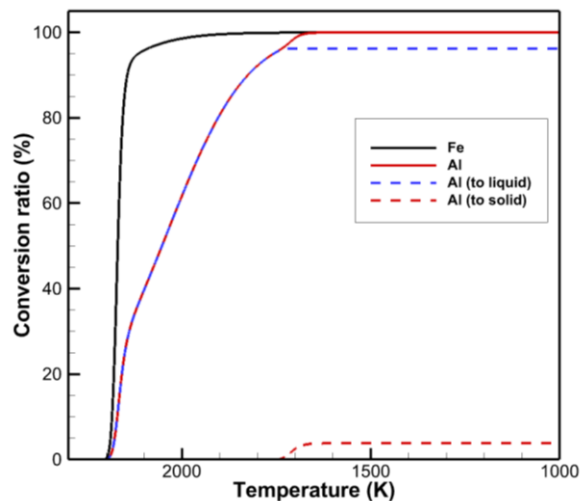


Fig. 3. Conversion ratios of Fe and Al vapors.

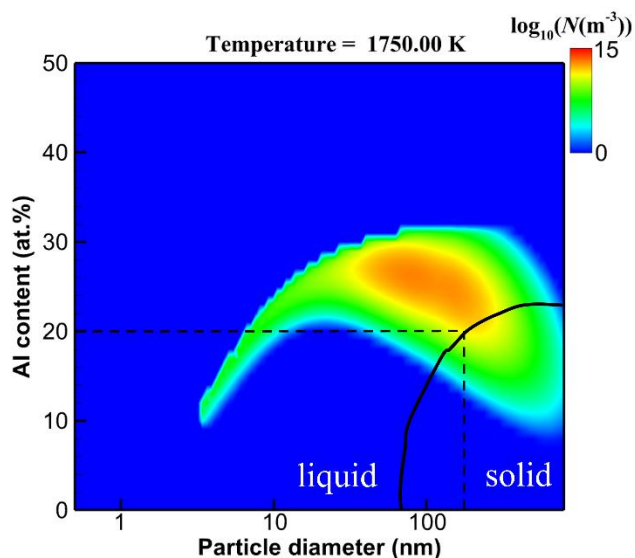


Fig. 4. Number density distribution of Fe-Al alloy particles at 1750 K.

condensed on solid particles at temperature lower than 1750 K, and condensed on liquid particles at higher temperature.

5. References

- [1] Y. B. Pithawalla et al., *Journal of Physical Chemistry B*, **105**, 11, 2085-2090 (2001).
- [2] M. Shigeta and A. B. Murphy, *Journal of Physics D: Applied Physics*, **44**, 174025 (2011).
- [3] T. Watanabe, H. Okumiya, *Science and Technology of Advanced Materials*, **5**, 639-646 (2004).
- [4] M. Shigeta and T. Watanabe, *Journal of Applied Physics*, **108**, 043306 (2010).
- [5] G. Guisbiers et al., *Journal of Physical Chemistry C*, **112**, 11, 4097-4103 (2008).
- [6] T. B. Massalski et al., Vol. 3, ASM International (1990).